Holocene volcanic history as recorded in the sulfate stratigraphy of the European Project for Ice Coring in Antarctica Dome C (EDC96) ice core

E. Castellano, Silvia Becagli, M. Hansson, M. Hutterli, J.-R. Petit, M. R. Rampino, M. Severi, J. P. Steffensen, Rita Traversi, Roberto Udisti

Holocene volcanic history as recorded in the sulfate stratigraphy of the European Project for Ice Coring in Antarctica Dome C (EDC96) ice core

E. Castellano,[1] S. Becagli,[1] M. Hansson,[2] M. Hutterli,[3] J. R. Petit,[4] M. R. Rampino,[5] M. Severi,[1] J. P. Steffensen,[6] R. Traversi,[1] and R. Udisti[1]

[1] A detailed history of Holocene volcanism was reconstructed using the sulfate record of the European Project for Ice Coring in Antarctica Dome C (EDC96) ice core. This first complete Holocene volcanic record from an Antarctic core provides a reliable database to compare with long records from Antarctic and Greenland ice cores. A threshold method based on statistical treatment of the lognormal sulfate flux distribution was used to differentiate volcanic sulfate spikes from sulfate background concentrations. Ninety-six eruptions were identified in the EDC96 ice core during the Holocene, with a mean of 7.9 events per millennium. The frequency distribution (events per millennium) showed that the last 2000 years were a period of enhanced volcanic activity. EDC96 volcanic signatures for the last millennium are in good agreement with those recorded in other Antarctic ice cores. For older periods, comparison is in some cases less reliable, mainly because of dating uncertainties. Sulfate depositional fluxes of individual volcanic events vary greatly among the different cores. A volcanic flux normalization (volcanic flux/Tambora flux ratio) was used to evaluate the relative intensity of the same event recorded at different sites in the last millennium. Normalized flux variability for the same event showed the highest value in the 1100–1500 AD period. This pattern could mirror changes in regional transport linked to climatic variations such as slight warming stages in the Southern Hemisphere (Southern Hemisphere Medieval Warming–like period?).

1. Introduction

[2] Polar ice sheets are extensive sources of information on past atmospheric composition. Snow accumulated layer by layer and gradually compressed into solid ice in the coldest areas of ice sheets contains traces of atmospheric aerosol at the time of deposition. A major record coming from ice cores is the history of past explosive volcanism, reconstructed by electric conductivity measurements (ECM) [e.g., *Hammer et al.*, 1997] and sulfate ice core profiles [e.g., *Zielinski*, 2000].

[1]Department of Chemistry, University of Florence, Florence, Italy.
[2]Department of Physical Geography and Quaternary Geology, Stockholm University, Stockholm, Sweden.
[3]Physics Institute, University of Bern, Bern, Switzerland.
[4]Laboratoire de Glaciologie et Géophysique de l'Environnement du CNRS, Saint-Martin-d'Heres Cedex, France.
[5]Earth and Environmental Science Program, New York University, New York, New York, USA.
[6]Department of Geophysics, Niels Bohr Institute, University of Copenhagen, Copenhagen, Denmark.

[3] Volcanic eruptions emit large amounts of particulate matter and gases into various levels of the atmosphere, depending on eruption intensity and magma composition [*Rampino and Self*, 1982]. Explosive eruptions inject ash and gases (mainly SO_2) directly into the stratosphere, where they are transported on a regional to global scale [*Coffey*, 1996]. Aerosol microdroplets of sulfuric acid, formed by atmospheric oxidation of SO_2 and gas-to-particle conversion, have stratospheric lifetimes of months to a few years, affecting the Earth's radiative balance and climate and perturbing the chemistry of the stratosphere. The global distribution of volcanic aerosols was confirmed by satellite observation [e.g., *Hofmann et al.*, 2003], and its positive (warming) or negative (cooling) climatic effects have been largely discussed. *Robock* [2000] and *Zielinski* [2000] noted that stratospheric sulfate aerosol can affect regional or global climate through: (1) reduction of the diurnal temperature cycle, (2) stratospheric heating, (3) tropospheric cooling, and (4) perturbation of seasonal temperatures (summer cooling and winter warming). Megaeruptions or high-frequency events may speed up global climate changes acting as climate driving forces [*Budner and Cole-Dai*, 2003].
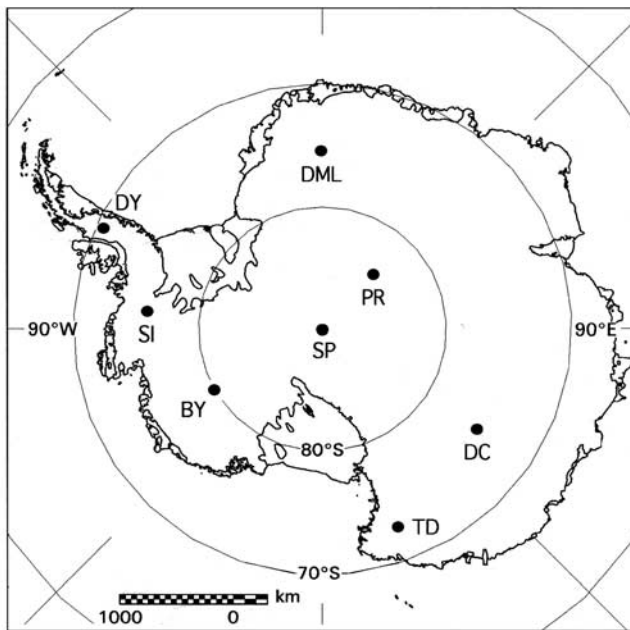
Figure 1. Map of Antarctica with location of cited drilling sites. Abbreviations are as follows: BY, Byrd; DC, Dome C; DML, Dronning Maud Land; DY, Dyer Plateau; LD, Law Dome; PR, Plateau Remote; SI, Siple Dome; SP, South Pole; TD, Talos Dome. References are reported in the text.

[4] Volcanic sulfate aerosols and ash are irreversibly deposited on polar ice sheets [*Clausen et al.*, 1997; *Delmas et al.*, 1992; *Hammer et al.*, 1997; *Langway et al.*, 1995; *Zielinski et al.*, 1994]. Sulfate ice core stratigraphy can be used to evaluate the stratospheric load of sulfate and obtain information on the climatic impact of explosive eruptions. This is not an easy task. Indeed, the deposition of volcanic SO_4^{2-} on ice sheets is affected by the geographic location of sources, the pattern of tropospheric/stratospheric exchange, seasonal features of atmospheric circulation [*Zielinski*, 2000; *Coffey*, 1996], and depositional processes (such as the relative contribution of dry and wet deposition, snow accumulation rate, and snowfall frequency). Finally, postdepositional effects such as wind scouring can affect records. To overcome these difficulties in the reconstruction of volcanic history, the ice core database on volcanic eruptions must be enlarged as much as possible and should consider regional features of sites located in the same ice sheet areas. Different transport pathways, also acting on a regional scale (as pointed out by *Udisti et al.* [2004]), can lead to different depositional fluxes for the same volcanic eruption.

[5] In many cores, volcanic stratigraphy was inferred by continuous acidity records from ECM [*Hammer et al.*, 1980, 1997; *Clausen et al.*, 1997] or dielectric profiling (DEP) [*Barnes et al.*, 2002; *Wolff et al.*, 1999]. However, the original acidic load can be partially or totally neutralized in the atmosphere or after deposition by buffering effects (e.g., by dust and ammonia). In contrast, since sulfate is irreversibly deposited on snow, records are insensitive to snow acidity changes; volcanic spikes are therefore more

easily distinguished from background values [*Udisti et al.*, 2000; *Cole-Dai et al.*, 1997].

[6] The volcanic stratigraphy at Dome C (DC, East Antarctica) was obtained from continuous sulfate measurements carried out on the EDC96 ice core drilled in the framework of the European Project for Ice Coring in Antarctica (EPICA). This is the longest paleovolcanic series from an Antarctic ice core. In a previous paper [*Castellano et al.*, 2004] we discussed the method used to discriminate volcanic signatures from background values and the eruption frequency recorded at DC for the last 45 kyr. Here we focus on the Holocene (0–11.5 kyr BP) volcanic record (first 360 m of the EDC96 ice core) characterizing all the volcanic signatures (dating, maximum sulfate concentration, and sulfate volcanic flux). The EDC96 volcanic data set can be used for interhemispheric and intrahemispheric comparison with other ice core–based volcanic records both to synchronize ice core stratigraphies and to study depositional processes of volcanic products. In this paper we focus on the comparison with previously published records from other Antarctic ice cores in terms of event frequency and intensity of the signatures. The spatial variability in the deposition of single events over the Antarctic ice sheet was evaluated by comparing normalized sulfate fluxes. Normalization was carried out by dividing volcanic fluxes by the Tambora flux in different Antarctic sites. We discuss whether changes in volcanic deposition and variability are possibly linked to changes in transport pathways driven by climatic variations.

2. Methods and Procedures
2.1. Ice Core Sampling and Analysis

[7] DC (75°06′S; 123°24 E; 3233 m a.s.l.) (Figure 1, showing all borehole locations cited in the text) was the site chosen in the framework of the EPICA program to obtain an ice core of more than 3000 m, which will yield paleoclimatic and paleoenvironmental information on about the last 900 kyr [*European Project for Ice Coring in Antarctica (EPICA) Dome C 2001–2002 Science and Drilling Teams*, 2002; *EPICA Community Members*, 2004]. Some details of the drilling site and of ice core processing have been published previously [*Tabacco et al.*, 1998; *Wolff et al.*, 1999; *EPICA Dome C 2001–2002 Science and Drilling Teams*, 2002]. Here we present data from the first 360 m of the EDC96 ice core, covering the entire Holocene (0–11.5 kyr BP). Owing to the poor quality of the first 6 m of ice core, the uppermost data were obtained by analyzing samples collected in a 7-m-deep snow pit dug during the 2000–2001 field season about 3 km from the main borehole.

[8] Ice core sulfate measurements were performed in the field by fast ion chromatography (FIC). FIC was carried out by coupling an ion-chromatographic method with a flow-injection analysis apparatus [*Udisti et al.*, 2000]. This method was set up to perform one analysis per minute of chloride, nitrate, and sulfate records in samples coming from a melter device: ice core sections were continuously melted after removal of a few mm of ice from core ends and possible breaks [*Röthlisberger et al.*, 2000]. The FIC temporal resolution (yr sample^{-1}) was calculated by multi-
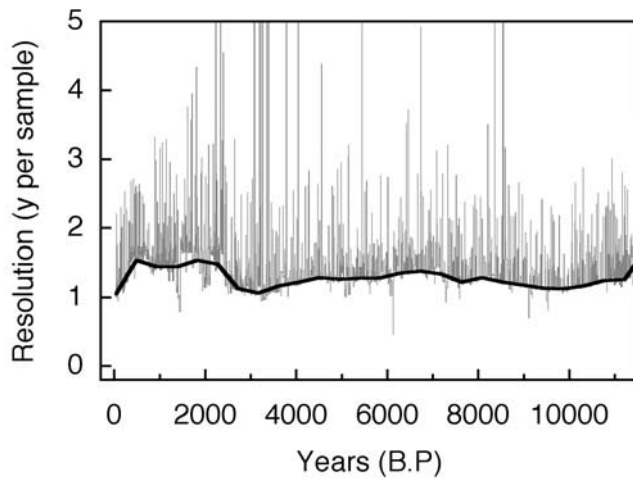
Figure 2. Temporal resolution of FIC data during the Holocene. Despite some outliers (data corresponding to a greater number of years due to breaks in the core and missing ice), the black smoothing curve shows that the temporal resolution for the Holocene ranges between about 1 and 1.5 years.

plying the measurement rate (1 min sample^{-1}) with the melting rate (4.0–7.0 cm min^{-1}) and dividing by the accumulation rate (2.50–2.56 cm yr^{-1} water equivalent (w.e.) [*Schwander et al.*, 2001]. The resolution is nearly annual in the Holocene, with values ranging from 1 to 1.5 yr sample^{-1}. Figure 2 shows the time resolution of FIC measurements versus age. The low-resolution spikes (up to 5 yr sample^{-1}) are numerically insignificant (around 2%) compared to the total sample number and are caused by ice loss during the decontamination of ice core bar extremities and possible breaks. The scarce relevance of the low-resolution spikes is demonstrated by the trend of the 200-year smoothed curve (dark line). A rather constant time resolution for superficial or deep ice core sections was obtained by melting them at different rates (7.0–4.0 cm min^{-1}) according to density.

[9] The accuracy of the FIC measurements was assessed by comparing chloride, nitrate, and sulfate FIC profiles with data obtained by classical ion chromatographic (IC) analysis of discontinuous samples at a similar resolution [*Littot et al.*, 2002]. Figure 3 shows the FIC and IC sulfate profiles around three volcanic spikes recorded at about 38 and 39 m (Figure 3a) and at 353 m (Figure 3b). Although background trends and peak shapes fit very well, there are some differences in absolute concentrations, especially for the 353 m spike (the FIC and IC Y scales were shifted for better comparison). For all the compared peaks, a mean standard deviation of about 10% was found between IC and FIC measurements. This uncertainty is very close to the internal reproducibility (5–10%) of FIC and IC. Furthermore, one must bear in mind that volcanic depositions are revealed by high sulfate concentrations, for which reproducibility is better than 5%.

2.2. Dating of Volcanic Events

[10] The EDC96 timescale (EDC1) [*Schwander et al.*, 2001] was obtained using a simple ice-flow model, with

accumulation rates derived from δD measurements and calibrated and confirmed by: (1) well-dated time horizons, such as known volcanic eruptions over the last 700 years; (2) matching between EDC96 and Vostok volcanic signatures from 1200 to 7100 years BP used to transfer a dated Vostok ice core sequence (through a link between ^{10}Be in ice and ^{14}C) to EDC96; (3) the synchronization between the CH_4 event at the end of the Antarctic Cold Reversal (ACR) and of the Greenland Younger Dryas (YD); (4) a sharp F^- signal dated to about 17,500 BP (recovered for the first time in the Byrd BS68 ice core by *Hammer et al.* [1997]); and (5) the estimated depth and age of a ^{10}Be peak (about 41 kyr BP). The EDC1 age uncertainty for the Holocene is estimated to be ±10 years from 0 to 700 years BP and as much as ±200 years up to 10 kyr BP. For the first part of the core (the last millennium), which contains a record of many historically well-known volcanic events, we compared the EPICA sulfate record with published ice core data sets, paying particular attention to data from ice cores drilled at sites where the annual snow accumulation rate allows stratigraphic dating (Byrd, Law Dome, Siple Dome, Dyer Plateau, and Talos Dome). Unambiguous and well-dated volcanic signatures (Agung-1964, Tambora-1816, Huaynaputina-1601, Kuwae-1460 and an unknown event dated 1259) were used to date the last 1000 years more accurately through polynomial interpolation of the five temporal horizons; this was then used to date other volcanic signatures. The new dating was compared with EDC1. Age differences
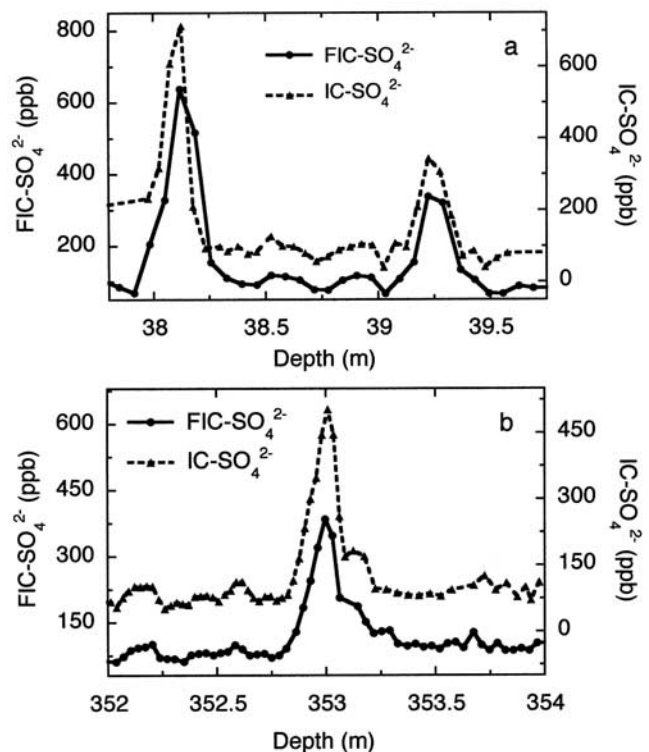

Figure 3. Comparison between FIC and discontinuous IC measurements in two selected sections of the EDC96 ice core showing three volcanic signatures dated (a) 1259 and 1230 AD and (b) 9212 BC.

Table 1. List of Events Recorded in the DC Ice Core for the Last Millennium[a]

Event	Depth, m	Year AD (EDC1 Model)	Year AD (This Work)	ΔAge	Maximum SO_4^{2-} Concentration, $\mu g\ l^{-1}$	Volcanic Flux, $kg\ km^{-2}$	Volcanic Eruption	F_{ev}/F_b
A	0.64	-	1992	-	313.2	10.7	Pinatubo + Hudson	0.57
B	2.95	-	1964	-	362.5	8.4	Agung	0.71
1	8.00	1894	1887	7	140.0	3.1	Krakatua	0.24
2	8.35	1888	1881	7	289.4	9.3	Cotopaxi	0.72
3	9.54	1868	1861	7	138.8	4.1	Makjan-Cotopaxi-Fuego	0.60
4	12.34	1820	1816	4	605.7	39.3	Tambora	1.96
5	12.68	1814	1807	7	270.5	10.2	unknown 1809	0.71
6	15.36	1764	1758	6	173.6	4.5	Jorullo-Taal	0.87
7	18.62	1700	1696	4	184.6	8.8	Serua	1.07
8	19.70	1678	1675	3	141.8	5.3	Gamkonora	0.61
9	22.20	1625	1624	1	174.6	8.0	Subantarctic	0.61
10	23.20	1603	1601	2	193.6	13.4	Huaynaputina	0.68
11	28.90	1473	1480	−7	182.4	9.5	?	0.47
12	29.77	1453	1460	−7	398.6	31.7	Kuwae	1.23
13	34.55	1341	1347	−6	211.4	10.4	?	0.69
14	36.96	1283	1288	−5	257.5	22.4	?	0.93
15	37.64	1267	1271	−4	304.2	20.5	?	1.18
16	38.12	1255	1259	−4	637.1	60.4	?	2.46
17	39.22	1228	1230	−2	336.9	25.2	?	1.28
18	40.79	1189	1190	−1	226.8	18.0	?	0.85
19	41.52	1171	1170	1	310.8	20.8	?	1.14

[a]The age of events was calculated using both the EDC1 dating model [*Schwander et al.*, 2001] and a fitting of major volcanic events (see text for further details). Volcanic fluxes and F_{ev}/F_b values were calculated as explained in the text. The attribution of sources was made referring to previously published works, mainly *Simkin and Siebert* [1994].

(reported in Table 1) are always less than 10 years, confirming the error estimation of *Schwander et al.* [2001].

2.3. Nonvolcanic Background and Detection of Events

[11] In order to reconstruct a reliable record of volcanic events recorded in the EDC96 ice core, it was necessary to evaluate the nonvolcanic sulfate background and set a threshold above which spikes can be attributed to volcanic deposition. The discrimination method used for the EDC96 ice core has already been discussed [*Castellano et al.*, 2004]; an outline of the method is here reported.

[12] Nonvolcanic sulfate contributions in Antarctic snow come from sea-salt spray, crustal erosion, and atmospheric oxidation of biogenic dimethylsulphide (DMS) [*Saltzman*, 1995; *Prospero et al.*, 1991]. The sea-salt sulfate contribution to total sulfate budget at DC in the Holocene, evaluated using Na^+ as a specific marker [*Legrand and Delmas*, 1988; *Röthlisberger et al.*, 2002], is less than 5%. The Holocene crustal contribution, calculated by non-sea-salt Ca^{2+} as a continental dust marker [*Röthlisberger et al.*, 2002], is even lower (<0.05%). Since these contributions are of the same order of measurement reproducibility, we did not correct sulfate concentrations and will not distinguish between sulfate and non-sea-salt sulfate in the following discussion.

[13] Discrimination between background and volcanic peaks was achieved by setting a variable threshold as follows [*Castellano et al.*, 2004]:

[14] 1. The distribution of sulfate concentrations and fluxes in the ice is more appropriately described by a lognormal instead of Gaussian distribution.

[15] 2. The variability of sulfate background concentrations (about $93 \pm 34\ \mu g\ l^{-1}$) is relatively large even in the Holocene (Figure 4a). Such variability could be caused by slight changes in the accumulation rate and/or in biogenic inputs, in turn due to changes in source intensity or in transport pathways of marine air masses. Since DC sulfate depositions are dominated by dry deposition [*Legrand and*

Delmas, 1987], the effect of variable snow accumulation rates can be corrected by considering the sulfate flux (calculated by multiplying concentration by the accumulation rate expressed in water equivalents) instead of concen-
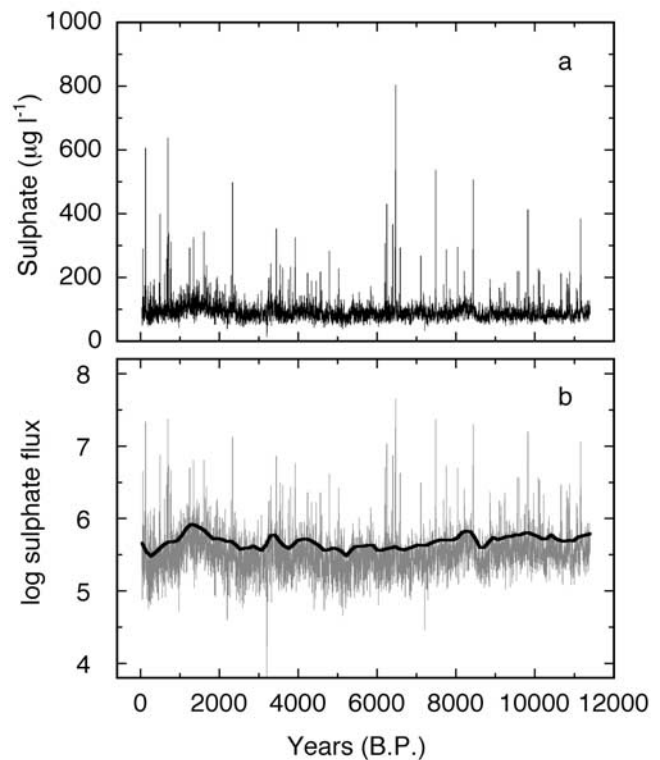

Figure 4. (a) Holocene profiles of sulfate concentrations and (b) the logarithm (neperian) of sulfate flux. The bold line in Figure 4b is the threshold curve used to distinguish between volcanic spikes and background sulfate concentrations.

Table 2. List of Events Recorded in the DC Ice Core for the Period 1000 AD to 9500 BC[a]

Event	Depth, m	Year AD (EDC1 Model)	Age, years BP (EDC1 Model)	Maximum SO_4^{2-} Concentration, $\mu g\ l^{-1}$	Volcanic Flux, kg km^{-2}	F_{ev}/F_b
20	51.54	926	1024	173.5	7.8	0.52
21	57.83	765	1185	179.3	7.9	0.40
22	60.42	699	1251	292.6	33.0	1.18
23	64.20	601	1349	324.4	25.1	0.83
24	69.15	467	1483	187.1	7.3	0.35
25	73.58	340	1610	343.4	24.2	0.98
26	74.88	302	1648	200.5	12.0	0.46
27	75.79	276	1674	237.3	16.5	0.62
28	76.56	253	1697	165.9	10.1	0.62
29	76.85	245	1705	168.8	8.7	0.54
30	78.02	210	1740	180.9	6.8	0.45
31	79.49	166	1784	183.9	10.9	0.40
32	85.10	−2	1952	201.2	11.4	0.57
33	91.49	−200	2150	177.5	14.0	0.60
34	96.04	−348	2298	206.0	8.8	0.49
35	97.12	−384	2334	497.3	32.2	1.36
36	100.04	−482	2432	155.8	5.8	0.52
37	126.57	−1351	3301	201.9	6.6	0.34
38	126.85	−1361	3311	243.2	7.8	0.40
39	130.78	−1496	3446	352.4	26.6	1.36
40	133.84	−1598	3548	239.9	17.7	0.95
41	135.60	−1657	3607	228.7	11.5	0.71
42	140.01	−1804	3754	160.9	5.4	0.41
43	140.30	−1814	3764	193.6	8.6	0.64
44	141.56	−1858	3808	232.8	13.4	0.74
45	144.93	−1975	3925	324.2	28.1	1.06
46	153.91	−2288	4238	212.5	11.0	0.68
47	156.78	−2389	4339	187.9	8.4	0.47
48	160.18	−2509	4459	188.3	10.6	0.61
49	163.16	−2615	4565	216.7	7.8	0.55
50	164.16	−2651	4601	160.4	7.2	0.58
51	169.44	−2842	4792	282.5	17.6	0.89
52	175.24	−3049	4999	145.5	10.6	0.73
53	176.14	−3081	5031	227.3	14.3	1.15
54	190.26	−3593	5543	152.9	6.9	0.58
55	198.76	−3892	5842	171.8	7.0	0.49
56	200.32	−3949	5899	141.7	5.2	0.28
57	208.75	−4255	6205	306.0	41.6	1.18
58	209.90	−4297	6247	429.7	36.0	1.99
59	213.19	−4420	6370	169.6	9.6	0.52
60	214.00	−4450	6400	365.8	24.7	1.55
61	215.72	−4514	6464	534.8	37.1	2.36
62	215.94	−4523	6473	803.0	61.5	3.27
63	219.00	−4639	6589	292.6	16.9	0.96
64	232.75	−5161	7111	266.7	15.3	0.69
65	234.45	−5228	7178	151.6	5.7	0.49
66	234.74	−5239	7189	141.4	5.0	0.43
67	238.99	−5389	7339	141.1	7.8	0.57
68	243.33	−5538	7488	536.1	52.5	1.29
69	249.29	−5738	7688	178.0	6.6	0.55
70	251.40	−5809	7759	286.1	18.3	0.98
71	253.93	−5896	7846	163.1	3.8	0.64
72	259.44	−6094	8044	295.3	20.3	0.86
73	264.16	−6265	8215	218.4	14.1	0.64
74	270.59	−6490	8440	505.9	38.1	0.94
75	283.15	−6919	8869	194.6	10.5	0.47
76	290.18	−7155	9105	166.9	8.7	0.70
77	291.37	−7194	9144	154.7	7.6	0.39
78	294.14	−7283	9233	167.9	10.1	0.67
79	304.39	−7609	9559	218.5	14.3	0.76
80	305.70	−7650	9600	218.6	19.8	1.24
81	311.08	−7822	9772	152.5	6.7	0.32
82	312.86	−7878	9828	411.7	33.7	1.63
83	317.52	−8024	9974	175.7	9.3	0.40
84	321.15	−8141	10091	226.9	10.2	0.78
85	322.05	−8171	10121	218.4	14.7	0.57
86	325.31	−8277	10227	176.6	9.4	0.79
87	338.68	−8719	10669	212.0	9.1	0.78
88	339.40	−8743	10693	128.9	5.2	0.25
89	342.82	−8861	10811	195.9	11.4	0.66
90	343.74	−8893	10843	177.5	10.1	0.47
91	344.97	−8935	10885	217.2	24.4	0.81

Table 2. (continued)

Event	Depth, m	Year AD (EDC1 Model)	Age, years BP (EDC1 Model)	Maximum SO_4^{2-} Concentration, $\mu g \ l^{-1}$	Volcanic Flux, kg km^{-2}	F_{ev}/F_b
92	350.08	−9112	11062	164.9	6.4	0.41
93	350.80	−9136	11086	156.8	8.0	0.45
94	353.00	−9212	11162	383.4	41.0	1.42

[a]The age of events was calculated using the EDC1 dating model [*Schwander et al.*, 2001] and BP means before 1950. Volcanic fluxes and F_{ev}/F_b values were calculated as explained in the text.

trations. Sulfate flux calculation was carried out using highly resolved accumulation rates derived from δD measurements (resolution of 55 cm, corresponding to about 15 years in the Holocene) [*Schwander et al.*, 2001] coupled with a simple one-dimensional thinning model (dome location). The residual variability in the sulfate flux background is described by a curve obtained by a 3% weighted fit smoothing procedure on the log-flux profile. This smoothing function fits a curve to data using the locally weighted (in this case 3% of total data) least squared error method. The result is to plot a best fit smooth curve through the center of data. This is an extremely robust fitting technique nearly insensitive to outliers. The final curve used as the threshold between volcanic spikes and sulfate background concentrations was obtained by adding 2 log σ to the log-flux smoothed profile, as shown in Figure 4b.

[16] 3. In order to reject outliers leading to false positives, we decided to subjectively evaluate volcanic signature peaks consisting of only one sample above the threshold.

[17] We thus detected 96 volcanic events in the first 360 m of the EDC96 core, which covers the Holocene period (0–11.5 kyr BP); volcanic signatures are listed in Tables 1 and 2 along with glaciological parameters (depth, age, and flux).

[18] Different peak detection algorithms have been presented in previous works [e.g., *Cole-Dai et al.*, 1997; *Zielinski et al.*, 1994]. When comparing volcanic records from different ice cores, one must bear in mind that the number of detected events closely depends on the selected detection method. Nevertheless, differences among the various methods are supposed to affect only minor volcanic signatures just above or below the threshold, while major global eruptions (characterized by higher climatic impact) are insensitive to differences in detection strategy, assuming that other factors such as regional variability and postdepositional effects did not influence volcanic deposition.

2.4. Volcanic Fluxes

[19] Accurate sulfate fluxes for each volcanic peak (integrated net depositional volcanic flux expressed in kg km^{-2}) were calculated by subtracting the sulfate background concentration from the total sulfate concentration in each sample recording the specific volcanic event. The residual was multiplied by the sample length and density; the total flux was calculated by summing single sample contributions [*Cole-Dai and Mosley-Thompson*, 1999]. The sulfate background flux for each volcanic spike was calculated as the mean short-period background value of 5 samples before and after the volcanic peak. EDC96 densities in the firn were measured directly. Since sulfate analysis was carried out in a continuous way, sample lengths correspond to the mean melting rate of ice core sections in each depth interval. Postdepositional effects due to diffusion or snow-layer

mixing processes affect concentrations but not fluxes [*Barnes et al.*, 2003]. However, wind redistribution could affect both, even leading to the complete removal of snow layers recording a volcanic event.

[20] A reliable evaluation of sulfate volcanic fluxes allows a more accurate estimation of the relative contribution of two possible climatic forcings linked to the global sulfur cycle acting on different atmospheric scales: the stratosphere (volcanic inputs) and troposphere (biogenic emissions). Tables 1 and 2 show ratios between volcanic and background sulfate fluxes (F_{ev}/F_b) for each volcanic event. Volcanic events are characterized by concentration spikes, but their deposition lasts for a short time; as a consequence, in most cases, volcanic fluxes are lower than background values (mainly of biogenic origin) deposited in the same interval of time. Only a few major events show a F_{ev}/F_b ratio >1. For example, the Tambora eruption produced a total sulfate deposition at DC only about 2 times higher than the contemporaneous background contribution, although its concentration peak is about 6 times higher. The cumulative sulfate flux calculation may be used to evaluate the overall contribution of explosive volcanic activity to the total sulfate budget at DC. The high-resolution EDC96 sulfate record allows a reliable estimation of the total amount of background sulfate deposition during the entire Holocene, about 2.5 10^4 kg km^{-2}. Cumulative explosive volcanism contributes about 1.5 10^3 kg km^{-2}, corresponding to about 6% of the total sulfate budget.

3. Results and Discussion
3.1. Frequency of Volcanic Events

[21] Figure 5 shows the number of volcanic events per millennium recorded in the EDC96 ice core (black bars) during the Holocene. Volcanic frequencies from other Antarctic and Greenland ice cores, covering at least 1000 years, are also plotted. The average eruption number per millennium recorded at DC during the Holocene is 7.9, with oscillations between low- and high-frequency periods. In particular, the last millennium shows the highest eruption frequency in the whole record (21 eruptions), followed by 12 volcanic signatures in the 1000–0 AD period. As already pointed out by *Castellano et al.* [2004], the last two millennia are characterized by the greatest number of volcanic signatures in the whole 45-kyr volcanic record of EDC96. This finding is unlikely due to glaciological effects, such as different resolution or layer thinning; indeed, as mentioned in the methodology section, the temporal resolution of FIC measurements was kept essentially constant by adjusting the ice core melting rate to density variations, and the thinning effect in the uppermost 360 m is negligible [*Barnes et al.*, 2003]. The high frequency of signatures in the last 2000 years confirms the *Cole-Dai et al.* [2000]
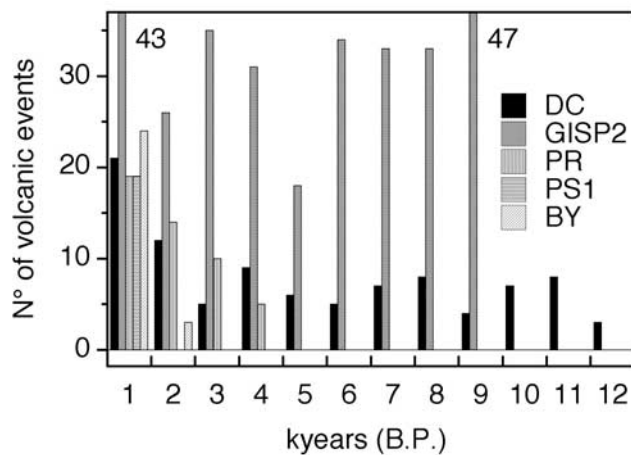
Figure 5. Frequency of volcanic events in the Holocene, expressed as number of events per millennium, for the DC, PR, PS1, BY, and GISP 2 ice cores. References are reported in the text.

measurements on the 4100-year ice core drilled at Plateau Remote (PR). This record lists 33 eruptions in the last 2000 years, with a millennium distribution similar to that observed at DC, 19 (last millennium) and 14 (penultimate millennium). To minimize the effect of the threshold choice on moderate volcanic signatures, we considered only depositions with fluxes higher than 20 kg km^{-2} (this value was chosen by *Cole-Dai et al.* [2000] as the limit between large and medium events). For these major signatures the two records give the same values: both PR and EDC96 ice cores show 10 and 3 large events recorded in the last 1000 years and in the previous millennium, respectively. The high frequency of volcanic signatures recorded in the Antarctic ice sheet during the last millennium is confirmed by other shorter-interval ice core records: 18 events in ~550 years at Siple Station (SI) [*Cole-Dai et al.*, 1997]; 15 events in ~400 years at Dyer Plateau (DY) [*Cole-Dai et al.*, 1997]; 23 events at the South Pole (SP-PS1 ice core) [*Delmas et al.*, 1992]; 25 events at Dronning Maud Land (DML) [*Karlöf et al.*, 2000]; and 25 events in ~1150 years at Byrd (BY-NB89 ice core) [*Langway et al.*, 1994]. The larger number of volcanic events recorded at SI and DY (Antarctic Peninsula) could be ascribed to the higher temporal resolution of sulfate measurements (linked to the higher accumulation rate), which can potentially permit to distinguish short time-spaced volcanic eruptions. In contrast, global events distributed by long-range transport (mainly via the stratosphere) are characterized by long (2–3 years) residence times of submicrometric sulfuric aerosol; therefore resolutions close to one sample per year (as in all Antarctic ice cores here discussed) seem to assure consistent results in event computation. Indeed, only very high resolutions (such as those obtained in Greenland and at coastal Antarctic sites) are really able to separate events which occurred only a few months apart. For this reason we consider more relevant the relative closeness of SI and DY sites to active volcanic systems (e.g., South Sandwich Island and Deception Island), highlighting the importance of local to regional events. Indeed, Figure 5 shows that the number of

events recorded in the Greenland GISP2 ice core [*Zielinski et al.*, 1996], with a mean frequency of 33.3 volcanic events per millennium during the Holocene (1000-year means ranging from 18 to 47 eruptions), is much greater than in Antarctic cores. As already discussed by *Cole-Dai et al.* [2000] and *Castellano et al.* [2004], the difference is not surprising, considering the relative closeness of Greenland to areas with a high density of active volcanic systems (e.g., Iceland, Kamchatka, etc.).

3.2. Comparison of the EDC96 Volcanic Profile With Other Antarctic Ice Cores

[22] Comparing volcanic fluxes recorded in ice cores from different sites is essential for reconstructing the spatial distribution of net deposition from single events, for understanding the impact of changes in atmospheric transport, and for evaluating the intensity of past volcanic eruptions and their possible influence on global climate. Furthermore, the synchronization of different ice cores using volcanic temporal horizons helps improve ice core dating. We present here a comparison of volcanic stratigraphies recorded in different Antarctic ice cores and discuss differences in depositional fluxes.

3.2.1. Comparison Among Antarctic Volcanic Stratigraphies

[23] Figure 6 compares the volcanic stratigraphy of the last millennium (volcanic sulfate flux versus age) recorded in the EDC96 ice core with that recorded in five other Antarctic ice cores on which sulfate measurements were carried out: BY, SP (PS1 ice core), PR, SI, and DY (see references in section 3.1). Data related to the EDC96 signatures are also reported in Table 1. As described in section 2.2, the age of DC events was calculated by interpolating five historically well-known volcanic eruptions. These events are recorded in all Antarctic ice cores covering the last 1000 years, and their signatures have been accurately dated in sites characterized by high annual snow accumulation rates [e.g., *Cole-Dai et al.*, 1997; *Palmer et al.*, 2001] or by using other dating techniques (e.g., dendrochronology and historical reports) [*Simkin and Siebert*, 1994]. Thanks to the closeness of temporal horizons, in this section of ice core, event ages are likely to be more accurate than those obtained from the ice flow model (EDC1).

[24] Although most of the sulfate spikes in the EDC96 ice core are also recorded in all other ice cores, there are some differences. The most relevant particularity is the number of peaks grouped in the so-called "1259 sequence" (13th century). This sequence, a series of events centered on the highest signature dated 1259 AD, is also recorded in Greenland ice cores [*Clausen et al.*, 1997]. Among the four Antarctic ice cores covering this time period (EDC96, BY, PS1, and PR), PR and BY show the complete series of five volcanic signatures, while PS1 only shows the three central events. In the EDC96 ice core the peak sulfate concentration of the signature dated 1276-8 is lower than the threshold (see section 2.3) and was not included in Figure 6 and Table 1. Finally, the highest peak of the "1259 sequence" in the PR ice core is the 1277 event. With the exception of the EDC96 1276-8 event (probably affected by wind scouring), these differences are unlikely due to the choice of different detection methods because all signatures are well above the threshold.
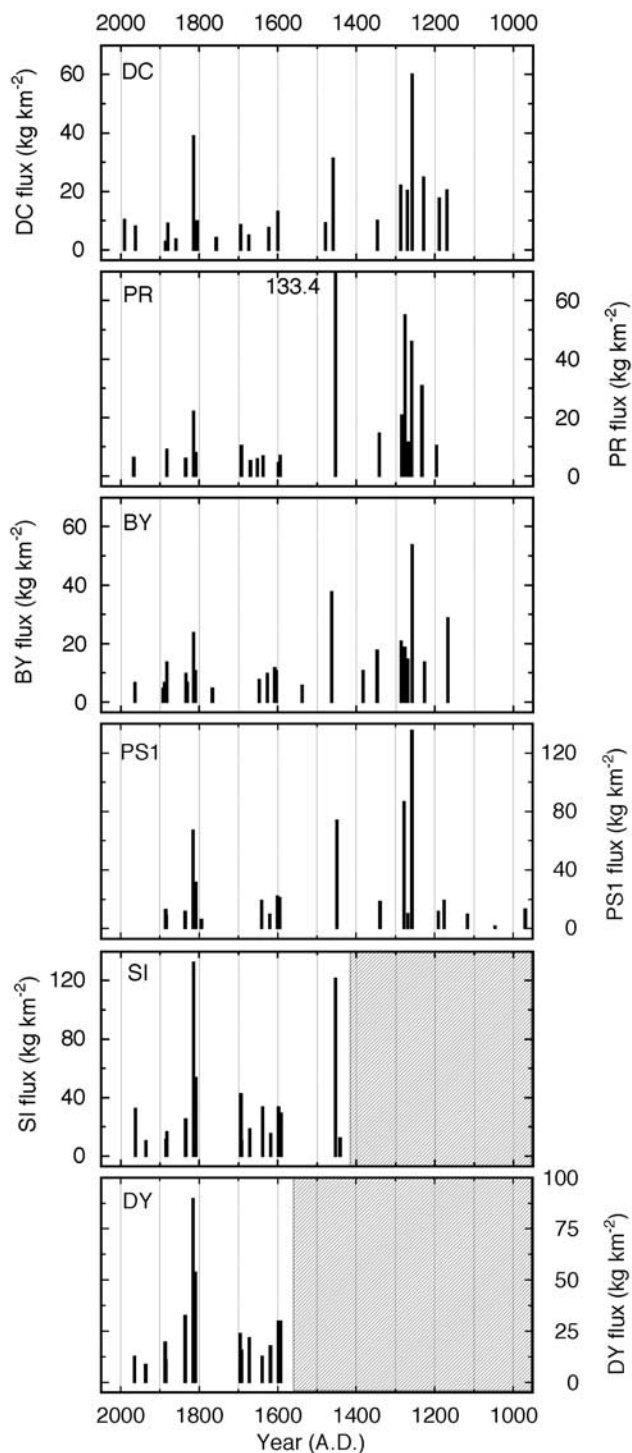
Figure 6. Comparison of volcanic profiles (volcanic flux versus age) for the last millennium from sulfate measurements in the DC, PR, BY, PS1, SI, and DY ice cores. References are reported in the text. In the PR plot, 133.4 is the out-of-scale flux value of the Kuwae signature. Shaded areas indicate periods not covered by ice cores.

[25] Minor signatures in cores are generally in agreement; only three minor volcanic events recorded in the EDC96 core are unmatched in the other records (peaks 3, 6, and 11 in Table 1, dated 1861, 1758, and 1480 AD, respectively),

but synchronous signatures were found in other shallow firn cores [*Legrand and Delmas*, 1987; *Cole-Dai and Mosley-Thompson*, 1999]. In contrast, two medium-intensity events, dated 1835-6 and 1593-5 and recorded in all the ice cores reported in Figure 6 (with the only exception of the oldest event in the BY core), are not present in the EDC96 stratigraphy. Nevertheless, these signatures show high fluxes only in ice cores drilled in coastal areas (SI and DY), while they are recorded as minor events in the PR core drilled on the East Antarctic Plateau. As discussed in the next section, differences in net depositional fluxes and the loss of minor peaks could be due to changes in atmospheric circulation processes and to local glaciological features (wind redistribution, relative contribution of wet-dry deposition, accumulation rates, and frequency and timing of snowfalls), particularly relevant in low-accumulation sites.

[26] Besides DC, the only other Antarctic volcanic stratigraphy extending back to more than 1000 AD comes from the PR ice core, which covers the last 4100 years. This volcanic profile is plotted in Figure 7a together with EDC96 stratigraphy (Figure 7b). Although in agreement over the last 1000 years, the two profiles look quite different in the older period. In particular, there is no correspondence between periods characterized by lack of volcanic signals in the two cores. In the period 500–1350 BC the DC ice core records no event, whereas the PR core contains 11 signatures, including three large events. However, in the period 1500–2000 BC, EDC96 recorded seven events, with two signatures showing sulfate fluxes higher than 20 kg km^{-2}; in the same temporal range, no volcanic signatures are recorded in the PR ice core. Another six events are recorded in the PR core in the 2000–2200 BC period without corresponding signatures in the EDC96 ice core. Differences are also seen in sections recording a similar numbers of volcanic events (e.g., in the penultimate millennium), making it difficult to compare major signatures also. Differences between PR and EDC96 volcanic signatures cannot be attributed to the poor quality of ice cores. The compared sections do not belong to the ''brittle zone,'' where fragile ice causes frequent breaks. As for ice-bar quality, previous works do not show evidence of poor quality in the PR core [e.g., *Cole-Dai et al.*, 2000]. Breaks in EDC96 affected only 2% of the ice core (see section 2.1), and the ice lost during decontamination of bar extremities before melting involved only 1–3 mm. In addition, there were no relevant differences in the number of volcanic peaks in sulfate and DEP or ECM stratigraphies [*Udisti et al.*, 2000, 2004] (the latter two were carried out on uncut, 2.2-m-long ice core bars). Besides changes in atmospheric patterns and glaciological features, relative shifts in the timescale of the two ice cores may account for the observed differences. Indeed, these cores were drilled in the East Antarctic Plateau, where low accumulation rates occur, and were dated with nonstratigraphic methods. An accurate peak-to-peak comparison between the volcanic signatures recorded at DC and VK in the last 45 kyr [*Udisti et al.*, 2004] revealed differences of up to 3500 years, highlighting the importance of volcanic stratigraphy in synchronizing different ice cores. A preliminary peak-to-peak comparison between volcanic signatures in the EDC96 and EDML ice cores (unpublished data) revealed the good fit between volcanic signatures recorded in the period 1000–7000 years BP in
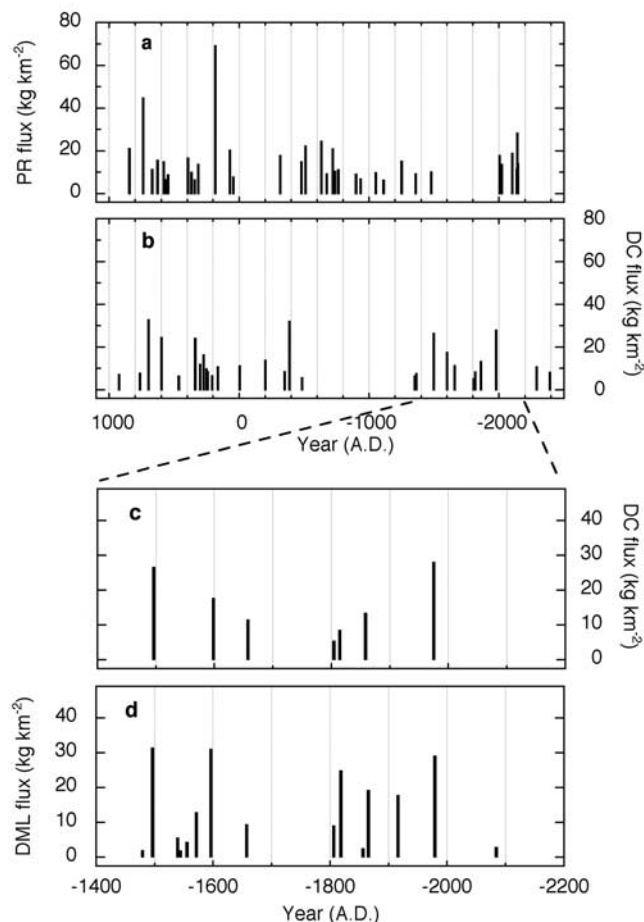
Figure 7. Comparison of volcanic profiles (volcanic flux versus age) from sulfate measurements in the (a) PR and (b) DC ice cores for the period 1000 AD to 2500 BC and in the (c) DML and (d) DC ice cores for the period 1450–2200 BC. In Figures 7c and 7d, age is calculated by the EDC1 dating model (see section 2.2).

sites located at opposite sides of Antarctica (data processing is still in progress). For example, Figures 7c and 7d compare EDC96 and EDML in the 1450–2200 BC period, when maximum differences where found between EDC96 and PR stratigraphies. Indeed, five of six major signatures are contemporaneous in EDC96 and EDML profiles, sustaining the reliability of the DC record. When EDML is finally dated (stratigraphic dating by counting annual layers), the absolute dating of the EDC96 volcanic signatures will be assessed. In any case, these comparisons clearly highlight the need to increase the number of ice core based volcanic stratigraphies in order to overcome the lack of single ice cores signatures.

3.2.2. Comparison of Depositional Fluxes

[27] Volcanic sulfate fluxes in the six ice cores (Figure 6) differ considerably over the last 1000 years. As mentioned earlier, several factors can account for differences, particularly regional features (e.g., variability in the atmospheric circulation, also related to the period of the year where the eruption happens) [*Robock*, 2000] and glaciological effects such as wind redistribution processes which are very efficient at low accumulation sites [*Petit et al.*, 1982]. The

Kuwae signature (1460 AD) is a major example of depositional spatial variability. This signature is by far the most intense in the PR volcanic record, while in the other cores the 1259 event always shows the highest sulfate deposition. *Cole-Dai et al.* [2000] tentatively explained the lower sulfate flux of the "1259 event" in the PR core as possibly due to a partial loss of sulfate deposition by wind scouring. However, in the Talos Dome (TD) ice core (see *Stenni et al.* [2002]; not reported in Figure 6), Kuwae is again by far the highest volcanic signature in the last 800 years. It therefore seems probable that differences in the Kuwae signature can be ascribed to a real spatial variability in its depositional fluxes.

[28] In order to objectively compare volcanic flux variability among the different sites, ice core signatures were normalized with respect to the 1816 AD Tambora eruption, as suggested by *Cole-Dai et al.* [1997], thereby correcting for regional features. Indeed, with few exceptions such as the Kuwae event, nonnormalized fluxes are always higher at coastal sites, where high accumulation rates are observed and wet deposition strongly contributes to sulfate atmospheric scavenging (see SI and DY in Figure 6). Normalization was carried out by dividing the sulfate flux of each volcanic event (F) by the Tambora flux (F_T) in each core. Assuming that depositional and postdepositional processes at individual sites did not differ significantly over a relatively short interval of time (the last 1000 years), Tambora-normalized fluxes should be less dependent on the glaciological features (accumulation rate, snowfall frequency and annual distribution, wind redistribution, etc.) of sampling sites [*Cole-Dai et al.*, 1997]. Normalized fluxes (F/F_T) measured in several ice and firn cores are reported in Figure 8 along with corresponding standard deviations (σ, vertical bars in Figure 8b). In addition to the previously listed ice cores, the figure also contains the following Antarctic firn cores: PS14 (South Pole; *Delmas et al.* [1992]), SP96 (South Pole; *Cole-Dai and Mosley-Thompson* [1999]) and TD (Talos Dome; *Proposito et al.* [2003]). Tambora-normalized values (Figure 8a) are constantly lower than 1 for all events which occurred after 1500 AD, while several events show higher values in the early last millennium. The variability of the F/F_T ratio among the different cores (standard deviation in Figure 8b) shows a similar pattern: very low values were observed for the most recent events and higher values for the oldest signatures. Consistent patterns (not shown here) were obtained through the use of signatures than Tambora as normalization reference; this evidence seems to exclude the possibility that F/F_T ratio scattering is partly due to an anomalous Tambora signature in some cores. Furthermore, the higher variability in the older period does not seem to be imputable to higher ratio values as the 1460 event might suggest. Indeed, events with the same ratios occurred in the 1400–1200 AD period, showing a significantly higher absolute standard deviation with respect to events which occurred in the more recent period. In addition, when a volcanic event other than Tambora is considered as reference for normalization, the Tambora/reference ratios show a low standard deviation in spite of the fact that Tambora is the largest signature in the last 500 years. Figure 8b shows that normalized ratios $\sigma < 0.1$ are usual for events that occurred after 1500 AD. Most volcanic events in the early
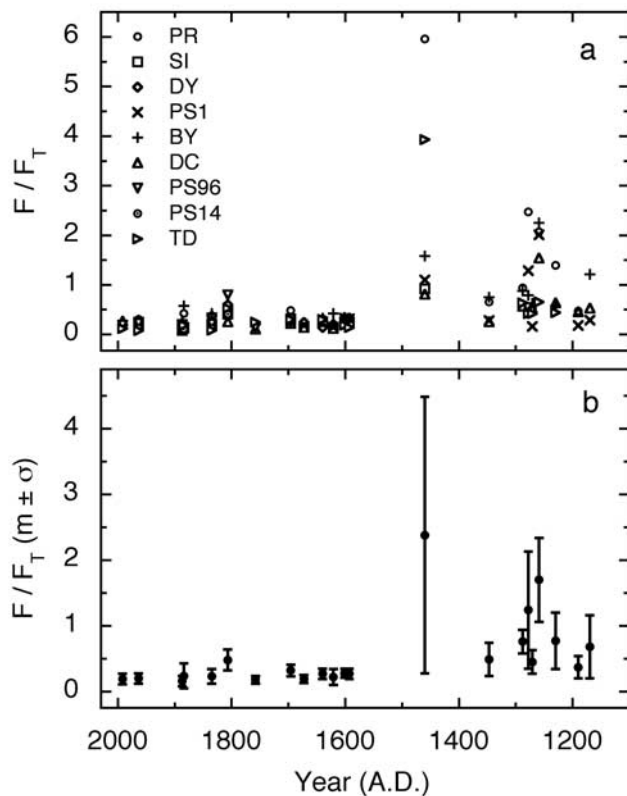
Figure 8. (a) The ratios between fluxes of events recorded in at least 4 of 9 Antarctic ice cores (PR, SI, DY, PS1, BY, DC, PS96, PS14, and TD) and Tambora (used as reference event) are reported against age for the last millennium. (b) The standard deviation for the considered events is indicated. References are reported in the text.

last millennium (1000–1500 AD), especially the Kuwae eruption ($F/F_T = 2.38 \pm 2.10$), show higher variability. Why do events which occurred in the 12th–16th centuries show large F/F_T ratios and higher variability? Of course, the higher Tambora-normalized signatures in the older period could be due to larger volcanic emissions [*Budner and Cole-Dai*, 2003]; they could have been more intense, for example, than some large modern volcanic events such as the Agung (1964) and Pinatubo (1991) eruptions, but this does not account for the larger variability. Local glaciological features, such as wind redistribution, changes in accumulation rate, and variations in the frequency and timing of snowfalls, could have affected the observed depositional variations. Considering that such effects should have been minimized by the adopted normalization procedure, we postulate that changes in atmospheric circulation driven by climate forcing on regional to global scales around Antarctica could have affected depositional processes in the 1000–1500 AD period. As suggested by *Budner and Cole-Dai* [2003], the Antarctic polar vortex is involved in the distribution of stratospheric volcanic aerosols over the continent. Assuming that the intensity and persistence of the polar vortex (both in the troposphere and stratosphere) mainly affect the penetration of air masses to inland Antarctica, isolating the continental area during cold periods and facilitating the advection of peripheral air masses during warm

periods [*Krinner and Genthon*, 1998], we support the hypothesis that the pattern of volcanic deposition intensity and geographical variability could reflect a warmer climate of Antarctica in the early last millennium. The re-establishment of colder conditions, starting in about 1500 AD, reduced the variability of volcanic depositions. This warm/cold step could be like a Medieval Climate Optimum–like to Little Ice Age–like transition. Medieval Warming is well defined in the Northern Hemisphere by several proxies [e.g., *O'Brien et al.*, 1995; *Wilson et al.*, 2000], while no clear evidence has been reported for Austral regions [*Dahl-Jensen et al.*, 1999]. In a recent paper, *Goosse et al.* [2004, and references therein] report evidence from δD and $\delta^{18}O$ measurements on Antarctic ice cores in support of a Medieval Warming–like period in the Southern Hemisphere, delayed by about 150 years with respect to Northern Hemisphere Medieval Warming. We postulate that changes in the extent and intra-Antarctic variability of volcanic depositional fluxes may have been consequences of the establishment of a Medieval Warming–like period that lasted until about 1500 AD. The re-establishment of mean Holocene climate conditions (or, perhaps of Little Ice Age–like conditions) increased the insulation of the Antarctic continent by increasing the intensity and persistence of the tropospheric and stratospheric polar vortex. These climatic conditions could have forced air masses containing sulfuric aerosol to follow longer pathways around Antarctica, thereby leading to more homogeneous deposition over the continent.

[29] Such changes in atmospheric transport processes could be similar (but to a lower extent) to that proposed by *Delmonte et al.* [2002] and *Udisti et al.* [2004] to explain variations in dust deposition and accumulation rates at DC during the different climatic conditions in the last 45 kyr. In the coldest periods (especially the Last Glacial Maximum) the higher intensity and persistence of the polar vortex prevented the direct advection of air masses to central areas of Antarctica, thereby sorting the size of atmospheric particles and homogenizing accumulation rates.

4. Conclusions

[30] The complete volcanic history of the Holocene was reconstructed using the EDC96 high-resolution sulfate record. A total of 96 eruptions were identified in the last 11,500 years, with a mean of 7.9 events per millennium. The last 2000 years were characterized by enhanced volcanic activity (21 events in the last millennium and 12 events in the penultimate millennium).

[31] The comparison between EDC96 and other volcanic records from Antarctic ice cores highlighted some implications in the use of ice core data for reconstructing volcanic history. Our study revealed two major constraints: (1) for the oldest sections of the cores (4000–2000 BP), where dating of ice layers is not straightforward, reliable synchronization of ice core timescales must be performed before sulfate signatures belonging to the same volcanic event can be compared; (2) for more recent periods, the comparison among signatures of single volcanic events recorded in ice cores drilled in different Antarctic sites reveals the high variability in sulfate depositional fluxes, even when these are normalized with respect to a well characterized eruption (e.g., Tambora event, 1816 AD).

[32] Regional features (accumulation rate, frequency and annual distribution of snowfalls, wind redistribution) and changes in atmospheric transport considerably affect the extent and distribution of volcanic deposition on the ice sheet. A Medieval Warming–like period could therefore be responsible for the observed increase in volcanic flux extent and dispersion.

[33] The atmosphere-to-snow exchange process models (formulated in the past based on total beta activity data from stratospheric fallout after thermonuclear tests; *Clausen and Hammer* [1988]) have to be improved through the introduction of variables linked to changes in atmospheric transport processes. This would improve the reliability of estimates of the impact of past volcanism on climate, based on sulfate fluxes in ice cores.

[34] In this context, high-resolution sulfate profiles from the two EPICA deep ice cores at Dome C (EDC; 3200 m in the 2002/2003 campaign) and Dronning Maud Land (EDML; 2500 m in the 2003/2004 campaign) and from a new Italian-French deep drilling project at Talos Dome (Ross Sea Region, to begin in the 2004/2005 austral summer) will increase the number and temporal extension of Antarctic volcanic stratigraphies, thereby providing new tools for investigating the relationship between volcanism and climate.

References

Barnes, P. R. F., E. W. Wolff, R. Mulvaney, R. Udisti, E. Castellano, R. Röthlisberger, and J.-P. Steffensen (2002), Effect of density on electrical conductivity of chemically laden polar ice, *J. Geophys. Res.*, 107(B2), 2029, doi:10.1029/2000JB000080.

Barnes, P. R. F., E. W. Wolff, H. M. Mader, R. Udisti, E. Castellano, and R. Röthlisberger (2003), Evolution of chemical peak shapes in the Dome C, Antarctica, ice core, *J. Geophys. Res.*, 108(D3), 4126, doi:10.1029/2002JD002538.

Budner, D., and J. Cole-Dai (2003), The number and magnitude of large explosive volcanic eruptions between 904 and 1865 A. D.: Quantitative evidence from a new South Pole ice core, in *Volcanism and the Earth's Atmosphere*, *Geophys. Monogr. Ser.*, vol. 139, edited by A. Robock and C. Oppenheimer, pp. 165–176, AGU, Washington, D. C.

Castellano, E., S. Becagli, J. Jouzel, A. Migliori, M. Severi, J. P. Steffensen, R. Traversi, and R. Udisti (2004), Volcanic eruption frequency in the last 45 kyr as recorded in EPICA-Dome C ice core (East Antarctica) and its relationship to climate changes, *Global Planet. Change*, 42, 195–205.

Clausen, H. B., and C. U. Hammer (1988), The Laki and Tambora eruptions as revealed in Greenland ice cores from 11 locations, *Ann. Glaciol.*, 10, 16–22.

Clausen, H. B., C. U. Hammer, C. S. Hvidberg, D. Dahl-Jensen, J. P. Steffensen, J. Kipfstuhl, and M. Legrand (1997), A comparison of the volcanic records over the past 4000 years from the Greenland Ice Core Project and Dye 3 Greenland ice cores, *J. Geophys. Res.*, 102(C12), 26,707–26,723.

Coffey, M. T. (1996), Observations of the impact of volcanic activity on stratospheric chemistry, *J. Geophys. Res.*, 101(D3), 6767–6780.

Cole-Dai, J., and E. Mosley-Thompson (1999), The Pinatubo eruption in South Pole snow and its potential value to ice-core paleovolcanic records, *Ann. Glaciol.*, 29, 99–105.

Cole-Dai, J., E. Mosley-Thompson, and L. G. Thompson (1997), Annually resolved southern hemisphere volcanic history from two Antarctic ice cores, *J. Geophys. Res.*, 102(D14), 16,761–16,771.

Cole-Dai, J., E. Mosley-Thompson, S. P. Wight, and L. G. Thompson (2000), A 4100-year record of explosive volcanism from an East Antarctica ice core, *J. Geophys. Res.*, 105(D19), 24,431–24,441.

Dahl-Jensen, D., V. I. Morgan, and A. Elcheikh (1999), Monte Carlo inverse modelling of the Law Dome (Antarctica) temperature profile, *Ann. Glaciol.*, 29, 145–150.

Delmas, R. J., S. Kirchner, J. M. Palais, and J. R. Petit (1992), 1000 years of explosive volcanism recorded at the South Pole, *Tellus, Ser. B*, 44, 335–350.

Delmonte, B., J. R. Petit, and V. Maggi (2002), Glacial to Holocene implications of the new 27,000 year dust record from the EPICA Dome C (East Antarctica) ice core, *Clim. Dyn.*, 18, 647–660.

European Project for Ice Coring in Antarctica (EPICA) Community Members (2004)Eight glacial cycles from an Antarctic ice core, *Nature*, 429, 623–628.

European Project for Ice Coring in Antarctica (EPICA) Dome C 2001–2002 Science and Drilling Teams (2002), Extending the ice core record beyond half a million years, *Eos Trans. AGU*, 83, 45, 509, 517.

Goosse, H., V. Masson-Delmotte, H. Renssen, M. Delmotte, T. Fichefet, V. Morgan, T. van Ommen, B. K. Khim, and B. Stenni (2004), A late medieval warm period in the Southern Ocean as a delayed response to external forcing?, *Geophys. Res. Lett.*, 31, L06203, doi:10.1029/2003GL019140.

Hammer, C. U., H. B. Clausen, and W. Dansgaard (1980), Greenland ice sheet evidence of post-glacial volcanism and its climatic impact, *Nature*, 288, 230–235.

Hammer, C. U., H. B. Clausen, and C. C. Langway Jr. (1997), 50,000 years of recorded global volcanism, *Clim. Change*, 35, 1–15.

Hofmann, D., J. Barnes, E. Dutton, T. Deshler, H. Jäger, R. Keen, and M. Osborn (2003), Surface-based observations of volcanic emissions to the stratosphere, in *Volcanism and the Earth's Atmosphere*, *Geophys. Monogr. Ser.*, vol. 139, edited by A. Robock and C. Oppenheimer, pp. 57–73, AGU, Washington, D. C.

Karlöf, L., et al. (2000), A 1500 year record of accumulation at Amundsenisen western Dronning Maud Land, Antarctica, derived from electrical and radioactive measurements on a 120 m ice core, *J. Geophys. Res.*, 105(D10), 12,471–12,483.

Krinner, G., and C. Genthon (1998), GCM simulations of the Last Glacial Maximum surface climate of Greenland and Antarctica, *Clim. Dyn.*, 14, 741–758.

Langway, C. C., Jr., K. Osada, H. B. Clausen, C. U. Hammer, H. Shoji, and A. Mitani (1994), New chemical stratigraphy over the last millennium for Byrd Station, Antarctica, *Tellus, Ser. B*, 46(1), 40–51.

Langway, C. C., Jr., K. Osada, H. B. Clausen, C. U. Hammer, and H. Shoji (1995), A 10 century comparison of prominent bipolar volcanic events in ice cores, *J. Geophys. Res.*, 100, 16,241–16,247.

Legrand, M., and R. J. Delmas (1987), A 220-year continuous record of volcanic H_2SO_4 in the Antarctic ice sheet, *Nature*, 327, 671–676.

Legrand, M., and R. J. Delmas (1988), Soluble impurities in four Antarctic ice cores over the last 30,000 years, *Ann. Glaciol.*, 10, 116–120.

Littot, G. C., R. Mulvaney, R. Röthlisberger, R. Udisti, E. W. Wolff, E. Castellano, M. De Angelis, M. Hansson, S. Sommer, and J. P. Steffensen (2002), Comparison of analytical methods used for measuring major ions in the EPICA-Dome C (Antarctica) ice core, *Ann. Glaciol.*, 35, 299–305.

O'Brien, S. R., P. A. Mayewski, L. D. Meeker, D. A. Meese, M. S. Twickler, and S. I. Whitlow (1995), Complexity of Holocene climate as reconstructed from a Greenland ice core, *Science*, 270, 1962–1964.

Palmer, A. S., T. D. van Ommen, M. A. J. Curran, V. Morgan, J. M. Souney, and P. A. Mayewski (2001), High-precision dating of volcanic events (A.D. 1301–1995) using ice cores from Law Dome, Antarctica, *J. Geophys. Res.*, 106(D22), 28,089–28,095.

Petit, J. R., J. Jouzel, M. Pourchet, and L. Merlivat (1982), A detailed study of snow accumulation and stable isotope content in Dome C (Antarctica), *J. Geophys. Res.*, 87(C6), 4301–4308.

Proposito, M., R. Gragnani, O. Flora, L. Genoni, and M. Frezzotti (2003), Volcanic record at GPS1, GPS2, 31DPT and M2 stations along the 1998–99 ITASE traverse (East Antarctica), *Terra Antarct. Rep.*, 8, 61–66.

Prospero, J. M., D. L. Savoie, E. S. Saltzman, and R. Larsen (1991), Impact of oceanic sources of biogenic sulphur on sulfate aerosol concentrations at Mawson, Antarctica, *Nature*, 350, 221–223.

Rampino, M. R., and S. Self (1982), Historic eruptions of Tambora (1815), Krakatau (1883), and Agung (1963), their stratospheric aerosols, and climatic impact, *Quat. Res.*, 18, 127–143.

Robock, A. (2000), Volcanic eruption and climate, *Rev. Geophys.*, 38, 191–219.

Röthlisberger, R., M. Bigler, M. A. Hutterli, S. Sommer, B. Stauffer, H. G. Junghans, and D. Wagenbach (2000), Technique for continuous high-resolution analysis of trace substances in firn and ice cores, *Environ. Sci. Technol.*, 34, 338–342.

Röthlisberger, R., R. Mulvaney, E. W. Wolff, M. A. Hutterli, M. Bigler, S. Sommer, and J. Jouzel (2002), Dust and sea salt variability in central

East Antarctica (Dome C) over the last 45 kyrs and its implications for southern high-latitude climate, *Geophys. Res. Lett.*, *29*(20), 1963, doi:10.1029/2002GL015186.

Saltzman, E. S. (1995), Ocean/atmosphere cycling of dimethylsulfide, in *Ice-Core Studies of Global Biogeochemical Cycle*, *NATO ASI Ser.*, vol. 30, *Global Environmental Change*, edited by R. J. Delmas, pp. 65–89, Springer, New York.

Schwander, J., J. Jouzel, C. U. Hammer, J. R. Petit, R. Udisti, and E. W. Wolff (2001), A tentative chronology for the EPICA Dome Concordia ice core, *Geophys. Res. Lett.*, *28*(22), 4243–4246.

Simkin, T., and L. Siebert (1994), *Volcanoes of the World*, 2nd ed., Geoscience Press, Tucson, Ariz.

Stenni, B., M. Proposito, R. Gragnani, O. Flora, J. Jouzel, S. Falourd, and M. Frezzotti (2002), Eight centuries of volcanic signal and climate change at Talos Dome (East Antarctica), *J. Geophys. Res.*, *107*(D9), 4076, doi:10.1029/2000JD000317.

Tabacco, I. E., A. Passerini, F. Corbelli, and M. Gorman (1998), Determination of the surface and bed topography at Dome C, East Antarctica, *J. Glaciol.*, *44*(146), 185–191.

Udisti, R., S. Becagli, E. Castellano, R. Mulvaney, J. Schwander, S. Torcini, and E. W. Wolff (2000), Holocene electrical and chemical measurements from the EPICA-Dome C ice core, *Ann. Glaciol.*, *30*, 20–26.

Udisti, R., S. Becagli, E. Castellano, B. Delmonte, J. Jouzel, J. R. Petit, J. Schwander, B. Stenni, and E. W. Wolff (2004), Stratigraphic correlations between the European Project for Ice Coring in Antarctica (EPICA) Dome C and Vostok ice cores showing the relative variations of snow accumulation over the past 45 kyr, *J. Geophys. Res.*, *109*, D08101, doi:10.1029/2003JD004180.

Wilson, R. C. L., S. A. Drury, and J. L. Chapman (2000), *The Great Ice Age: Climate Change and Life*, Taylor and Francis, Philadelphia, Pa.

Wolff, E. W., I. Basile, J. R. Petit, and J. Schwander (1999), Comparison of Holocene electrical records from Dome C and Vostok, *Ann. Glaciol.*, *29*, 89–93.

Zielinski, G. A. (2000), Use of paleo-records in determining variability within the volcanism-climate system, *Quat. Sci. Rev.*, *19*, 417–438.

Zielinski, G. A., P. A. Mayewski, L. D. Meeker, S. I. Whitlow, S. M. Twickler, M. Morrison, D. A. Meese, A. J. Gow, and R. B. Alley (1994), Record of volcanism since 7000 B.C. from the GISP2 Greenland ice core and implications for the volcano-climate system, *Science*, *264*, 948–952.

Zielinski, G. A., P. A. Mayewski, L. D. Meeker, S. I. Whitlow, and M. S. Twickler (1996), A 110,000-yr record of explosive volcanism from the GISP2 (Greenland) ice core, *Quat. Res.*, *45*, 109–118.

————————

S. Becagli, E. Castellano, M. Severi, R. Traversi, and R. Udisti, Department of Chemistry, University of Florence, Via della Lastruccia 3, I-50019 Florence, Italy. (udisti@unifi.it)

M. Hansson, Department of Physical Geography and Quaternary Geology, Stockholm University, S-10691 Stockholm, Sweden.

M. Hutterli, Physics Institute, University of Bern, Sidlerstrasse 5, CH-3012 Bern, Switzerland.

J. R. Petit, Laboratoire de Glaciologie et Géophysique de l'Environnement du CNRS, 54 rue Moliere, BP 96, F-38402 Saint-Martin-d'Heres Cedex, France.

M. R. Rampino, Earth and Environmental Science Program, New York University, 100 Washington Square East, Room 1009, New York, NY 10003, USA.

J. P. Steffensen, Department of Geophysics, Niels Bohr Institute, University of Copenhagen, Juliane Maries Vej. 30, DK-2100 Copenhagen, Denmark.